Journal of Peptide Science
J. Peptide Sci. **11**: 104–112 (2005)
Published online 15 September 2004 in Wiley InterScience (www.interscience.wiley.com). DOI: 10.1002/psc.602

JOURNAL OF PEPTIDE SCIENCE

Peptides containing 4-amino-1,2-dithiolane-4-carboxylic acid (Adt): conformation of Boc-Adt-Adt-NHMe and NH···S interactions

ENRICO MORERA,[a] MARIANNA NALLI,[a] ADRIANO MOLLICA,[a] MARIO PAGLIALUNGA PARADISI,[a] MASSIMILIANO ASCHI,[b] ENRICO GAVUZZO,[c] FERNANDO MAZZA[b] and GINO LUCENTE[a]*

[a] Dipartimento di Studi Farmaceutici, Università di Roma 'La Sapienza' and Istituto di Chimica Biomolecolare, Sezione di Roma, CNR, 00185 Roma, Italy
[b] Dipartimento di Chimica, Ingegneria Chimica e Materiali, Università di L'Aquila, 67010 Coppito, L'Aquila, Italy
[c] Istituto di Cristallografia, CNR, CP 10, 00016 Monterotondo Stazione, Roma, Italy

Received 5 April 2004; *Accepted 18 May 2004*

Abstract: To study the conformational preferences induced by the insertion of the 4-amino-1,2-dithiolane-4-carboxylic acid (Adt) residue into a peptide backbone, the achiral N-protected dipeptide methylamide Boc-Adt-Adt-NHMe (**1**) was synthesized and its crystal state and solution conformation studied and compared with that exhibited by its carba-analogue Boc-Ac_5c-Ac_5c-NHMe containing two residues of 1-aminocyclopentane-1-carboxylic acid (Ac_5c). Compound **1** in the crystal adopts a type-III β-turn conformation and an analogous structure is that preferred in chloroform solution as established by ^{1}H-NMR and NOE information. In the crystal packing three different Adt rings form a cavity and the involved sulphur atoms give rise to unusual multiple interactions with one NH group. The chemical nature of these intermolecular and intramolecular main-chain···side-chain NH···S interactions are discussed in terms of quantum chemical calculations. Copyright © 2004 European Peptide Society and John Wiley & Sons, Ltd.

Keywords: conformation; crystal structure; C^α-tetrasubstituted α-amino acid; dithiolane amino acid; NH···S interactions; quantum chemical calculations; β-turns

INTRODUCTION

The alteration of the peptide backbone is a versatile and well established approach for obtaining synthetic models characterized by enhanced metabolic stability and a tendency to adopt predetermined secondary structures. In this context the exploitation of the properties of achiral and chiral α-amino acids possessing a quaternary α-carbon atom (C^α-tetrasubstituted α-amino acids) is being investigated extensively [1–6]. A number of theoretical and experimental studies deal with this subject and take into consideration, in addition to residues containing two linear side chains, the family of α-amino acids in which the C^α-carbon atom is part of a cycloaliphatic or heterocyclic ring [6, 7]. The use of C^α-tetrasubstituted amino acids containing a heterocyclic side chain is relatively more recent and provides the opportunity of combining the tendency to stabilize folded conformations with the chemical reactivity and the capability of establishing non-covalent interactions through the functionalities present in the side chain.

In the context of C^α-tetrasubstituted amino acids containing a heterocyclic side chain, the properties of synthetic peptides characterized by the presence of an unusual, albeit interesting, heterocyclic α-amino acid containing a quaternary α-carbon atom, namely 4-amino-1,2-dithiolane-4-carboxylic acid (Adt) was studied [8–11]. This achiral molecule contains a disulfide bridge forced inside a five-membered ring and it can be viewed as the oxidized form of a proteinogenic amino acid cysteine whose side chain has been doubled. It should be remembered that although 1,2-dithiolanes contain a disulfide bridge and are chemically related to the corresponding 1,3-dithiols they differ drastically from their open- or larger-chain disulfide counterparts in both their chemical reactivity and functions in biological systems [12, 13]. Although several synthetic and natural compounds containing the 1,2-dithiolane ring system are known and have been studied, including the biochemically relevant molecule lipoic acid [R(+)-1,2-dithiolane-3-pentanoic acid] [12, 14], the Adt amino acid residue was, until very recently, an exclusively synthetic building block [15, 16] whose introduction into the peptide backbone has been described in previous papers [8–11]. Rather surprisingly, the Adt residue has been very recently discovered by Appleton and Copp [17] in a dibrominated indole enamide, named 'kottamide E', isolated from the New Zealand ascidian *Pycnoclavella kottae*. This represents the first natural compound in which the presence of this conformationally restricted cysteine analogue has been found.

*Correspondence to: Gino Lucente, Dipartimento di Studi Farmaceutici, Università di Roma 'La Sapienza', P.le A. Moro 5, 00185 Roma, Italy; e-mail: gino.lucente@uniroma1.it

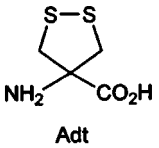

Adt

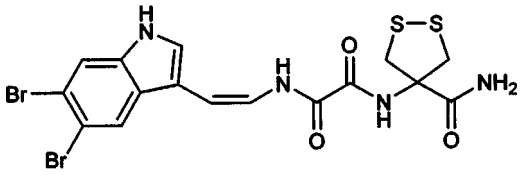

kottamide E

As a continuation of previous work on Adt containing peptides, this study reports the synthesis and conformational properties in solution and in the crystal state of the model dipeptide Boc-Adt-Adt-NHMe (Boc, *tert*-butyloxycarbonyl; NHMe, methylamide). The presence and nature of unusual multiple N–H···S interactions, as well as the relationship with the conformation adopted by the related N-Boc dipeptide methylamide containing two residues of 1-aminocyclopentane-1-carboxylic acid (Ac_5c) [18], are also discussed.

EXPERIMENTAL

Peptide Synthesis and Characterization

General. Melting points were determined with a Kofler hot-stage apparatus and are uncorrected. The IR absorption spectra were recorded in KBr (unless otherwise stated) employing a Perkin-Elmer FT-IR Spectrum 1000 spectrophotometer. The ^1H and ^{13}C NMR spectra were determined with an Avance 400 Bruker spectrometer using Me_4Si as the internal standard. 2D NOESY spectra were recorded on an Avance 400 Bruker console with a mixing time of 800, 1000 and 1200 ms and were displayed in the phase-sensitive mode. Integration of peak volumes was used to determine the relative NOE signals. Usually 256 × 1024 data points were collected and for each block 64 transients were collected for two dimensional experiments. The data sets were linearly predicted to 521 × 1024 data points. A sine window was applied in the F2 dimension and a sine squared window in the F1 dimension. Zero filling was used for a final spectrum size of 1024 × 1024 data points.

Column chromatography runs were carried out using Merck silica gel 60 (230–400 mesh). Thin-layer chromatography runs were performed on Merck 60 F_{254} silica gel plates. The drying agent was sodium sulfate. Boc-Adt-OMe (OMe, methoxy) was synthesized as previously reported [9]. The synthesis of Boc-Adt-Adt-NHMe (**1**) was performed in solution by adopting the conventional procedure, according to Figure 1.

Boc-Adt-OH. To a solution of Boc-Adt-OMe (0.100 g, 0.358 mmol) in methanol (MeOH) (1.5 ml) 2 M NaOH (0.36 ml) was added under stirring. After 12 h at room temperature, the solution was acidified with 0.5 M HCl, and extracted with ethyl acetate (EtOAc). The organic phase was washed with water, dried and evaporated to yield crude Boc-Adt-OH (0.093 g), which was used in the coupling step without further purification.

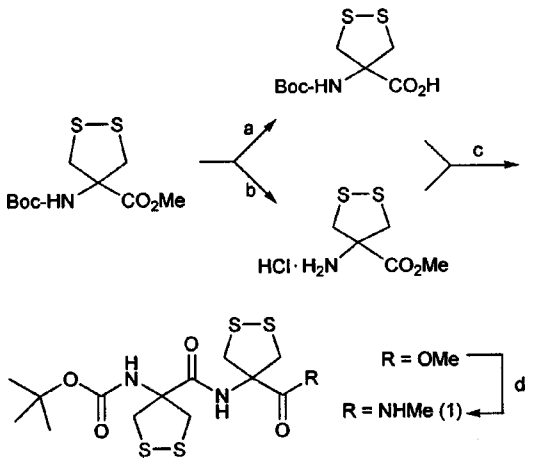

Figure 1 Synthesis of Boc-Adt-Adt-NHMe (**1**). a: NaOH 2 M, MeOH; b: $SOCl_2$, MeOH; c: HOBt, EDC, TEA, DMF; d: CH_3NH_2, MeOH.

HCl·H-Adt-OMe. To a solution of Boc-Adt-OMe (0.444 g, 1.59 mmol) in dry MeOH (10 ml) cooled to −15 °C, thionyl chloride (0.115 ml; 1.59 mmol) was added dropwise. After stirring at −15 °C for 30 min and at 50 °C for 5 h, the solution was evaporated under reduced pressure to give crude HCl·H-Adt-OMe. This salt was dissolved in dry MeOH, precipitated by the addition of dry diethyl ether, filtered and dried to give a white powder of HCl·H-Adt-OMe (0.253 g; 74%), which was used in the coupling step without further purification.

Boc-Adt-Adt-OMe. To a solution of Boc-Adt-OH (0.043 g, 0.16 mmol) in N,N-dimethylformamide (0.5 ml) cooled to 0 °C, 1-hydroxybenzotriazole (0.023 g, 0.17 mmol) and N-ethyl-N′-(3-dimethylaminopropyl)carbodiimide (0.033 g, 0.17 mmol) were added. After stirring for 15 min at 0 °C and for 20 min at room temperature, HCl·H-Adt-OMe (0.035 g, 0.16 mmol) and triethylamine (23 µl, 0.16 mmol) were added. The reaction mixture was stirred at room temperature for 18 h and then diluted with water and extracted with EtOAc. The organic phase was washed with water, 10% citric acid solution, saturated $NaHCO_3$ and water, and dried and evaporated under reduced pressure. The residue (0.061 g) was chromatographed on silica gel using *n*-hexane/EtOAc (7 : 3) as eluant to give 0.057 g (83%) of pure Boc-Adt-Adt-OMe. Melting point 188°–191 °C (from $CHCl_3$); $R_f = 0.40$ (*n*-hexane/EtOAc 6 : 4); IR (KBr) 3386, 3334, 1717, 1702, 1666 cm^{-1}; ^1H NMR (400 MHz, $CDCl_3$ + 10% CD_3OD); δ 1.46 (9H, s, *t*-butyl), 3.43 (4H, d, $J = 12.0$ Hz, Adt CH_2), 3.62 (2H, d, $J = 12.0$ Hz, Adt CH_2), 3.64 (2H, d, $J = 12.0$ Hz, Adt CH_2), 3.78 (3H, s, OCH_3), 5.58 (1H, s, urethane NH), 7.53 (1H, s, peptide NH); ^{13}C NMR (100 MHz, $CDCl_3$) δ 28.2 [$C(CH_3)_3$], 46.6, 47.4 (4 × CH_2S), 71.3, 71.6 [2 × $C(CH_2)_2$], 81.6[$C(CH_3)_3$], 154.5, 169.8, 171.9 (3 × CO).

Boc-Adt-Adt-NHMe. A solution of Boc-Adt-Adt-OMe (0.057 g, 0.134 mmol) in dry MeOH (2 ml) was saturated with dry CH_3NH_2 gas and kept tightly stoppered at room temperature for 5 days, at which time the conversion to the methylamide was deemed almost complete by TLC (CH_2Cl_2). Evaporation of the solvent afforded a crude residue (0.052 mg) which was chromatographed on silica gel (eluant CH_2Cl_2) to give 33 mg (58%) of pure Boc-Adt-Adt-NHMe as a powder. Melting

point 218°–219 °C (from MeOH); $R_f = 0.22$ (*n*-hexane/EtOAc 6 : 4); IR (KBr) 3336, 1698, 1652 cm^{-1}; ^1H NMR (400 MHz, $CDCl_3$) δ 1.48 (9H, s, *t*-butyl), 2.84 (3H, d, $J = 4.7$ Hz, $NHCH_3$), 3.28 (2H, d, $J = 12.4$ Hz, Adt^1CH_A), 3.51 (2H, d, $J = 12.0$ Hz, Adt^2CH_A), 3.70 (2H, d, $J = 12.4$ Hz, Adt^1CH_B), 3.72 (2H, d, $J = 12.0$ Hz, Adt^2CH_B), 5.51 (1H, s, urethane NH), 6.64 (1H, s, peptide NH), 7.49 (1H, br q, amide N*H*); ^{13}C NMR (100 MHz, $CDCl_3$) δ 26.9 ($NHCH_3$), 28.2 [$C(CH_3)_3$], 46.1, 46.6 ($4 \times CH_2S$), 71.5, 72.2 [$2 \times C(CH_2)_2$], 82.6[$C(CH_3)_3$], 156.0, 168.7, 168.8 ($3 \times CO$).

X-Ray Diffraction

Crystals of the title compound were obtained from methanol by slow evaporation. X-ray intensity data were collected on a Syntex $P2_1$ diffractometer equipped with graphite monochromatized Cu-kα radiation. Unit cell parameters refined on high angle reflections are reported in Table 1 together with details regarding data collection and structure refinement. The structure was solved by direct methods and refined using the package program SIR 2002 [19]. The non-H atoms were refined anisotropically by the full matrix least-squares method, including riding H atoms located at the expected positions with isotropic displacement parameters deduced from the carrier atoms. The correction for the real and imaginary parts of the anomalous dispersion was taken into account. In the last stages of refinement, the reflections $10\overline{1}$, 020 and 110 were excluded because they were judged severely affected by extinction. The final R and R_w values were 0.077 and 0.088, respectively. Crystallographic data (excluding structure factors) for the structure in this paper have been deposited with Cambridge Crystallographic Data Centre as supplementary publication CCDC-238 326. Copies of the data can be obtained, free of charge, on application to CCDC, 12 Union Road, Cambridge, CB2 1EZ, UK [fax: +44(0) 1223–336 033 or e-mail: deposit@ccdc.cam.ac.uk].

Table 1 Crystal Data for Boc-Adt-Adt-NHMe (**1**)

Empirical formula	$C_{14}H_{23}N_3O_4S_4$
Molecular weight	425.6
Crystal system	monoclinic
a (Å)	10.535(4)
b (Å)	20.696(6)
c (Å)	10.230(6)
β (°)	116.74(4)
V (Å^3)	1991(2)
Space group	$P2_1/n$
Calculated density (g/cm^3)	1.42
Z	4
F(000)	896
λ(Cu-kα) (Å)	1.5418
μ(Cu-kα) (mm^{-1})	4.42
Crystal size (mm)	$0.5 \times 0.2 \times 0.1$
$2\theta_{max}$(°)	124
Scan type	$\theta/2\theta$
No. reflections [$I > 3\sigma(I)$]	2895
No. refined parameters	226
Least-squares weight	$\sin\theta/\lambda$
R, R_w	0.077, 0.088
S	1.8

Quantum Chemical Calculations

The calculations were performed on the rings forming the cavity shown in Figure 5. In particular, for the reference molecule the model used was 4-formamido-1,2-dithiolane while for the other two symmetry related molecules unsubstituted 1,2-dithiolane rings were adopted. Their atomic coordinates were taken from the crystal structure. For this subsystem an overall ground state electronic wavefunction was optimized in the Hartree-Fock approximation using a standard split-valence 6-31+G (d, p) atomic basis set [20]. The eigenvalue of such a wavefunction, i.e. the potential energy of the subsystem, was decomposed through the standard Morokuma analysis [21]. The interaction energy (ET) was expressed as the sum of the following terms: ET = EES + EPL + ERE + ECT + EDI, where EES is the electrostatic contribution taking into account the interactions among the unperturbed charge distribution of the partners, EPL is the contribution arising from mutual polarization, ERE is the interpartner exchange repulsion, ECT is the interaction due to partial charge transfer from the HOMO of partner A to the LUMO of partner B and vice versa. The dispersion contribution (EDI) was subsequently evaluated using second order perturbation theory. To the above equation the effect of the basis set superposition error was also added [22]. The calculations were performed using the Gamess US package [23].

RESULTS AND DISCUSSION

Solution Conformation

To gain information on the conformational preferences of Boc-Adt-Adt-NH-Me (**1**) in solution, the chemical shift dependence of the NH resonances as a function of DMSO-d_6 concentration in $CDCl_3$ solution (10 mM) was studied (Figure 2). The assignment of the three NH groups in $CDCl_3$ is straightforward. The singlet at 5.51 ppm is assigned to the urethane Adt^1 NH by virtue of its high field position; the singlet at 6.64 ppm corresponds to the Adt^2 NH, while the broad quartet at 7.49 ppm is due to the methylamide NH group. As shown in Figure 2, the Adt^1 and Adt^2 NH groups are significantly more sensitive to changes in solvent composition compared with the methylamide NH group which appears strongly shielded. This behaviour clearly indicates that the methylamide NH group is not accessible to the solvent and is presumably involved in a $1 \leftarrow 4$ H-bond with the Boc C=O group in a β-turn conformation. The low field resonance of the –NHMe group is in agreement with this hypothesis. A comparison between the data on dipeptide **1** and those of the previously studied carba-analogue Boc-Ac_5c-Ac_5c-NH-Me [18] shows that the NH groups of the residues at the $(i + 2)$ position exhibit very distinct solvent exposures, expressed as differences ($\Delta\delta$, ppm) between the chemical shift values in $CDCl_3$ containing 10% DMSO-d_6 and in neat $CDCl_3$ (0.74 and ca. 0.15 ppm in the case of the Adt and Ac_5c, respectively). The lower solvent accessibility displayed by the Ac_5c

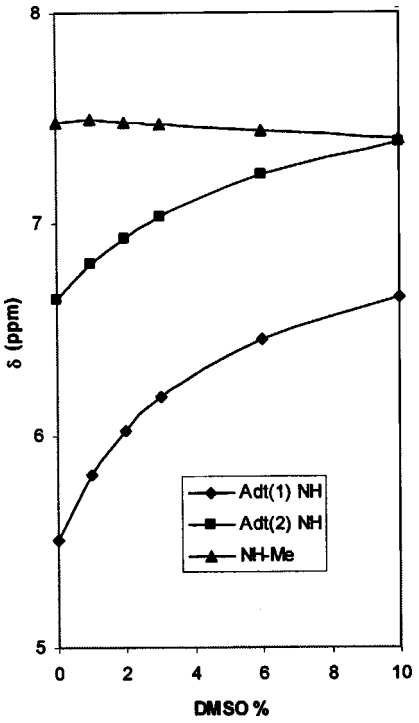

Figure 2 Plots of NH proton chemical shifts in the ^{1}H NMR of the peptide Boc-Adt-Adt-NHMe (**1**) as a function of increasing amounts of DMSO-d_6 (v/v) added to the $CDCl_3$ solution (peptide concentration: 10 mM).

NH group could be ascribed to a possible contribution of an $1 \leftarrow 3$ intramolecular H-bond between the Boc C=O and the Ac_5c NH in a γ-turn conformation [24]. This observation is in agreement with the results previously obtained in a conformational study on peptides containing Adt and Ac_5c amino acids, showing that the latter residue is more efficient as a γ-turn inducer [11].

Further information on the preferential solution conformation adopted by peptide **1** can be obtained by examining the results of nuclear Overhauser effect (NOE) experiments. However, the presence of two C^α-tetrasubstituted amino acids in peptide **1** and the consequent absence of the C^α H-atoms strongly limits the observation of the diagnostic interresidue connectivities.

The observed NOEs in the 2D NOESY spectra of **1** are summarized in Table 2 and Figure 3. These experiments allowed us to discriminate the four

Table 2 Observed Nuclear Overhauser Effects (NOEs) in the NOESY Spectra of Boc-Adt-Adt-NHMe (**1**)[a]

$Adt^1NH\cdots Adt^1CH_A$	s	$Adt^2NH\cdots Adt^2CH_A$	s
$Adt^1NH\cdots Adt^2NH$	m	$Adt^2NH\cdots NH$–Me	m
$Adt^2NH\cdots Adt^1CH_A$[b]	m	Adt^2CH_A[b] $\cdots NH$–Me	w

[a] s, strong; m, medium; w, weak.
[b] CH_A protons (see Figure 3) resonate at higher field than CH_B.

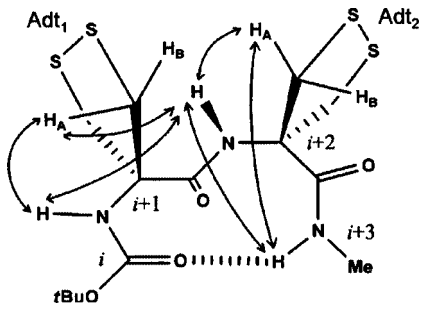

Figure 3 Relevant interproton correlations as deduced by NOESY experiments for Boc-Adt-Adt-NHMe (**1**).

doublets of the Adt^1 and Adt^2 methylene groups. The two enantiotopic protons, located on the same side of each dithiolane ring and facing the Adt NH, are in spatial proximity with this latter group and give rise, as expected, to the two strong intraresidue NOEs reported in Table 2. Thus, the two upfield doublets are assigned to the protons labelled as CH_A (3.28 and 3.51 ppm for Adt^1 and Adt^2, respectively) and the two downfield doublets (3.70 and 3.72 ppm for Adt^1 and Adt^2, respectively) are assigned to the protons labelled as CH_B which lie on the opposite side of the Adt NH and experience a selective deshielding effect by the adjacent carbonyl groups. NOEs pertaining to the Adt^1 and Adt^2CH_B protons have not been considered since the close proximity of their chemical shifts does not allow an unequivocal assignment of the spatial connectivities. The NOEs are useful in defining the preferred backbone conformation (Figure 3) involving the dithiolane ring NH groups and the methylamide NH. In particular, the occurrence of the cross interresidue peak $Adt^2NH\cdots MeNH$ is diagnostic of a β-turn conformation. Furthermore, the observation of a NOE between the NH protons of the two central residues, i.e. the Adt^1 and Adt^2 NH protons, rules out the occurrence of a significant population of type-II β-turn conformers and indicates a type I or a type III β-turn structure. This latter turn, which is similar to the type I, has been found in the crystal by x-ray diffraction analysis (see next section).

The IR absorption spectrum of **1** in 5.0 mM $CHCl_3$ solution shows a broad band centered at 3372 cm^{-1} in the stretching region of intramolecularly H-bonded N–H groups and no distinct absorption in the region where the band of free NH groups usually appears (ca. 3400–3450 cm^{-1}) [25, 26]. By operating at lower concentrations (1.0 and 0.3 mM in $CHCl_3$) no variations are observed in the spectrum, except for the appearance of two very weak absorptions centered at 3445 and 3435 cm^{-1}. This behaviour is different from that observed in the case of Boc-Ac_5c-Ac_5c-NHMe [18] which exhibits distinct absorptions centered at 3390–3400 cm^{-1} (H-bonded NH) and at 3440–3450 cm^{-1} (free NHs). Failure to observe the usually clearly differentiated band attributable to free NH

groups might be related to the presence in the relatively small molecule **1** of four electron rich sulfur atoms which can efficiently associate with polar NH groups [25, 27]. As a consequence, the purely free and H-bonded NH absorptions are not resolved and a broad single band is observed.

Crystal-state Conformation of Boc-Adt-Adt-NHMe (1)

The peptide backbone conformation found in the crystal can be described as a slightly distorted type-III β-turn stabilized by an $1 \leftarrow 4$ H-bond between the methylamide NH and the Boc C=O groups. A perspective view of the conformation, together with the adopted numbering scheme, is shown in Figure 4, while relevant torsion angles, describing backbone and side-chain conformations, are reported in Table 3. Since the achiral dipeptide crystallizes in a centrosymmetric space group, both type-III and type-III′ conformers are present in the crystal. The sign of the torsion angles reported in Table 3 refers to a type-III β-turn.

The Adt[1] and the Adt[2] residues, occupying the $(i+1)$ and the $(i+2)$ corner positions, respectively, adopt the following torsion angles: $\varphi_1 = -59.4^\circ(5)$, $\psi_1 = -32.5^\circ(4)$; $\varphi_2 = -68.3^\circ(4)$, $\psi_2 = -13.8^\circ(5)$. The φ_2 value is larger (10° ca.) and the ψ_2 value is smaller (15° ca.) than those expected for a type-III β-turn [28]. Also, the latter differs from that found [$-45.3^\circ(6)$] in the crystal of the peptide containing a single Adt residue Boc-Adt-OMe [8]. The bond angle N–C^α–C′ (τ), that is the most sensitive conformational parameter, always adopting tetrahedral or larger values in the folded forms of C^α-tetrasubstituted residues [29–31], is $111.2^\circ(4)$ and $111.9^\circ(4)$ for the $(i+1)$ and $(i+2)$ residues, respectively.

The ring conformation of the Adt[1] can be described as an envelope having the $S_1{}^{\gamma 2}$ sulfur at the flap. The other four ring atoms are coplanar to within 0.009 Å while $S_1{}^{\gamma 2}$ is out of the mean plane by 1.029(4) Å, and is oriented on the same side of the amino nitrogen N_1. The Adt[2] can be also described as an envelope, but the $C_2{}^{\beta 1}$ atom is at the flap. The other four ring atoms, including the disulfide bridge, are coplanar to within 0.001 Å, while the $C_2{}^{\beta 1}$ atom is out of the mean plane by 0.755(3) Å, and is oriented on the opposite side of the amino nitrogen N_2. Although the disulfide bridges have different torsion angles, $42.6^\circ(4)$ and $-24.9^\circ(2)$ for the $(i+1)$ and $(i+2)$ residues, they show bond length values of 2.066(4) Å and 2.073(3) Å, respectively, which are close to experimental error. The bond angles at the sulfur atoms of the Adt residue at the $(i+2)$ position [$92.6^\circ(2)$ and $96.4^\circ(2)$] are larger than those of the ring at $(i+1)$ [$89.4^\circ(3)$ and $93.9^\circ(3)$]. The former values can be related to the location of the disulfide bridge of Adt[2] in the plane of the other ring atoms.

The ring conformation and disulfide bond and torsion angles of the residue at the $(i+2)$ position are similar to those found in the crystal of Boc-Adt-OMe [8]. The Boc NH fragment is in the *trans-trans* planar conformation (ω_0 and θ^1 torsion angles -169.5° and -171.1°, respectively) with geometrical features in accordance with previous crystallographic findings for peptides containing this *N*-terminal protecting group [8, 32].

The backbone conformation of peptide **1** is similar to that adopted in the crystal by the previously studied carba-analogue Boc-Ac_5c-Ac_5c-NHMe [18]. This finding confirms that the insertion of constrained residues, containing five-membered rings into peptides, can stabilize β-turn conformations [33].

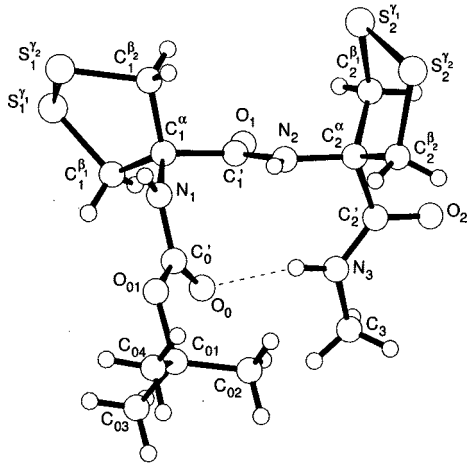

Figure 4 A perspective view of the Boc-Adt-Adt-NHMe (**1**) crystal conformation together with the adopted numbering scheme. Dashed line represents the intramolecular $1 \leftarrow 4$ H-bond.

Crystal Packing

In spite of their similar secondary structures, the Boc-Adt-Adt-NHMe model dipeptide (**1**) under study and Boc-Ac_5c-Ac_5c-NHMe [18] show marked differences in the aggregation mode giving rise to the crystal packing. Indeed, in the crystal of the carba-analogue the three NH groups are engaged in H-bonds with the three carbonyl oxygens; these are the $1 \leftarrow 4$ intramolecular and two intermolecular H-bonds between two symmetry related molecules, giving rise to H-bonded dimers. In the case of the Adt containing peptide **1** only two NH groups are engaged in interactions with carbonyl oxygens (one intra- and one intermolecular H-bond, as reported in Table 4). At variance, the N_1–H of the Adt at $(i+1)$ is engaged in several interactions with the surrounding electron-rich and polarizable sulfur atoms, as summarized in Table 5. Figure 5 is a stereoview, almost along the helical axis of the peptide, showing the aggregation found in the crystal packing, limited to the atoms surrounding the N_1–H group. This group lies in a cavity, elongated along the helical axis, where it is surrounded by three Adt rings belonging to three different molecules. These rings are indicated

Table 3 Main Torsion Angles (°) Found in the Crystal State for Boc-Adt-Adt-NHMe (**1**)

Backbone		Adt rings	
$C_{02}-C_{01}-O_{01}-C'_0$	54.5	$C^{\alpha}{}_1-C^{\beta 1}{}_1-S^{\gamma 1}{}_1-S^{\gamma 2}{}_1$	−28.9
$C_{03}-C_{01}-O_{01}-C'_0$	−72.0	$C^{\beta 1}{}_1-S^{\gamma 1}{}_1-S^{\gamma 2}{}_1-C^{\beta 2}{}_1$	42.6
$C_{04}-C_{01}-O_{01}-C'_0$	170.7	$S^{\gamma 1}{}_1-S^{\gamma 2}{}_1-C^{\beta 2}{}_1-C^{\alpha}{}_1$	−50.6
$C_{01}-O_{01}-C'_0-N_1$ (θ^1)	−171.1	$S^{\gamma 2}{}_1-C^{\beta 2}{}_1-C^{\alpha}{}_1-C^{\beta 1}{}_1$	38.3
$O_{01}-C'_0-N_1-C^{\alpha}{}_1$ (ω_0)	−169.5	$C^{\beta 2}{}_1-C^{\alpha}{}_1-C^{\beta 1}{}_1-S^{\gamma 1}{}_1$	−1.6
$C'_0-N_1-C^{\alpha}{}_1-C'_1$ (φ_1)	−59.4		
$N_1-C^{\alpha}{}_1-C'_1-N_2$ (ψ_1)	−32.5	$C^{\alpha}{}_2-C^{\beta 1}{}_2-S^{\gamma 1}{}_2-S^{\gamma 2}{}_2$	46.3
$C^{\alpha}{}_1-C'_1-N_2-C^{\alpha}{}_2$ (ω_1)	−176.5	$C^{\beta 1}{}_2-S^{\gamma 1}{}_2-S^{\gamma 2}{}_2-C^{\beta 2}{}_2$	−24.9
$C'_1-N_2-C^{\alpha}{}_2-C'_2$ (φ_2)	−68.3	$S^{\gamma 1}{}_2-S^{\gamma 2}{}_2-C^{\beta 2}{}_2-C^{\alpha}{}_2$	−0.1
$N_2-C^{\alpha}{}_2-C'_2-N_3$ (ψ_2)	−13.8	$S^{\gamma 2}{}_2-C^{\beta 2}{}_2-C^{\alpha}{}_2-C^{\beta 1}{}_2$	30.9
$C^{\alpha}{}_2-C'_2-N_3-C_3$ (ω_2)	178.4	$C^{\beta 2}{}_2-C^{\alpha}{}_2-C^{\beta 1}{}_2-S^{\gamma 1}{}_2$	−52.9

ESDs are 0.2–0.7°.

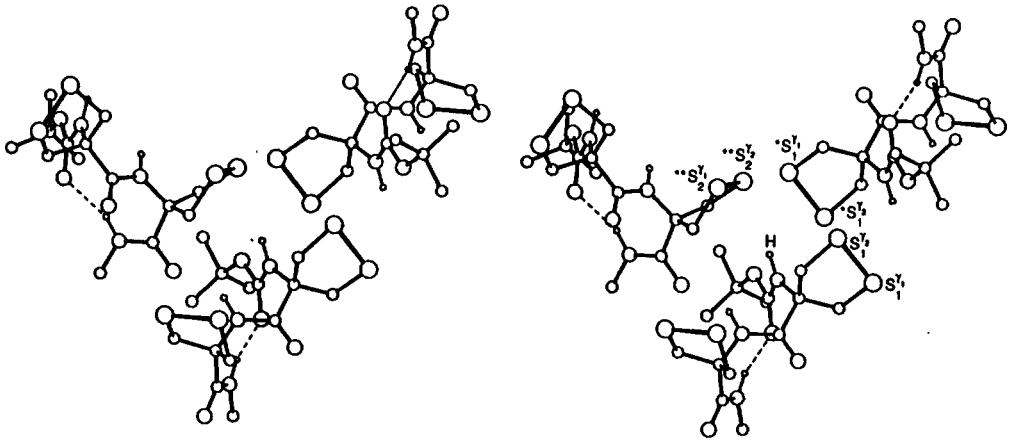

Figure 5 A stereoscopic view of the crystal packing cavity of Boc-Adt-Adt-NHMe (**1**) where the NH···S interactions take place. The hydrogen atom bound to N_1 and the disulfide bridges are indicated. The unstarred, single and double starred sulfur atoms are at the equivalent positions indicated in Table 5.

Table 4 Geometric Details of H-Bonds Found in the Crystal of Boc-Adt-Adt-NHMe (**1**)

Donor	Acceptor	D···A (Å)	H···A (Å)	D–Ĥ···A (°)
N_3	O_0	2.97	2.05	160.8
N_2	$O_2{}^{I}$	3.11	2.23	151.6

Symmetry code: I: $1/2+x$, $1/2-y$, $1/2+z$. ESDs are 0.005–0.01 Å and 0.3°–0.5°.

Table 5 Contacts (Å) and Angles (°) Formed between the N_1H Group of the Reference Molecule and the Surrounding Sulfur Atoms in the Cavity Shown in Figure 5

$N_1{}^{\cdots}S_1{}^{\gamma 1}$	3.771	$H^{\cdots}S_1{}^{\gamma 1}$	4.11	$N_1-\hat{H}^{\cdots}S_1{}^{\gamma 1}$	104
$N_1{}^{\cdots *}S_1{}^{\gamma 1}$	4.428	$H^{\cdots *}S_1{}^{\gamma 1}$	3.78	$N_1-\hat{H}^{\cdots *}S_1{}^{\gamma 1}$	127
$N_1{}^{\cdots}S_1{}^{\gamma 2}$	3.270	$H^{\cdots}S_1{}^{\gamma 2}$	3.11	$N_1-\hat{H}^{\cdots}S_1{}^{\gamma 2}$	91
$N_1{}^{\cdots *}S_1{}^{\gamma 2}$	3.818	$H^{\cdots *}S_1{}^{\gamma 2}$	3.60	$N_1-\hat{H}^{\cdots *}S_1{}^{\gamma 2}$	96
$N_1{}^{\cdots **}S_2{}^{\gamma 1}$	4.703	$H^{\cdots **}S_2{}^{\gamma 1}$	3.91	$N_1-\hat{H}^{\cdots **}S_2{}^{\gamma 1}$	141
$N_1{}^{\cdots **}S_2{}^{\gamma 2}$	3.780	$H^{\cdots **}S_2{}^{\gamma 2}$	2.83	$N_1-\hat{H}^{\cdots **}S_2{}^{\gamma 2}$	172

ESDs are 0.003–0.006 Å for the contacts of non H-atoms and 0.8°–1.2° for the angles.
Symmetry code: *: $2-x$, $1-y$, $1-z$. **: $-1/2+x$, $1/2-y$, $-1/2+z$.

by unstarred, single and double starred sulfur atoms. Their equivalent positions are given in Table 5. The unstarred and single starred Adt rings, both at the $(i+1)$ position, are parallel to each other and form the top and the bottom of the cavity, respectively. The double starred Adt ring, at the $(i+2)$ position, is intermediate between the two parallel rings with an orientation almost perpendicular to them and forms the wall of the cavity. In this situation the N_1 and the H atom bound to N_1 form intramolecular contacts of 3.270 (5) and 3.11(1) Å respectively, with the $S_1{}^{\gamma 2}$

atom, and intermolecular contacts of 3.780(6) Å and 2.827(1) Å, respectively, with the $^{**}S_2^{\gamma 2}$ atom. Both H···S contacts are shorter than their van der Waals radii sum. Moreover, the N–H···S angles are 91° and 172°, respectively, for the intramolecular and intermolecular interaction. These conditions favour H-bond formation which, as is well known [21], shows a non-negligible covalent character. This latter is maximized when the donor–acceptor angle approximates linearity and may be revealed by an exchange of a charge fraction between the atoms involved. The charge exchange can be quantitatively evaluated by analysing the quantum chemical nature of the bond.

Quantum Chemical Study of the NH···S Interactions

To understand more fully the nature of the NH···S interactions summarized in Table 5, a decomposition analysis was carried out of the potential energy computed for the simple subsystem formed by the amide N_1H group and the three rings forming the cavity. Quantum chemical calculations were performed as described in the Experimental section and the potential energy was decomposed by the Morokuma analysis [21], that is one of the most extensively adopted supermolecular decomposition approaches [34–36]. This method decomposes the interaction energy (ET) in the following components: electrostatic (EES), polarization (EPL), repulsive (EEX), charge transfer (ECT) and dispersion (EDI) terms. Table 6 reports the energy components obtained for the interaction that the amide N_1H group experiences with each of the three rings. It can be seen that the double starred Adt ring, forming the wall of the cavity, presents single contributions larger than those of the other two rings. The corresponding repulsive term results in 2.2 kcal/mol. If to this value the electrostatic and polarization terms, together giving −1.9 kcal/mol, are added, the interaction still remains repulsive. Only the inclusion of purely 'quantum' effects, namely the charge transfer and, most importantly, the dispersion term (evaluated as −1.2 and −2.1 kcal/mol, respectively), makes this interaction attractive. The interaction of the N_1H group with the other two rings have similar but lower energy components, contributing less than 50% to the global potential energy. However, even at larger distances, both dispersion and, to a minor extent, charge transfer appear as important cooperative terms.

In the light of the results of the above calculations, the main-chain··· side-chain intramolecular $N_1H\cdots S_1^{\gamma 2}$ and intermolecular $N_1H\cdots{}^{**}S_2^{\gamma 2}$ interactions cannot be considered simply electrostatic but, taking into account the quantum effects, they turn out to have a significant H-bond character. It should also be observed the cooperative character of these NH···S interactions concur to prevent the NH group from being an H-bond donor to a peptide carbonyl oxygen.

Table 6 Electrostatic (EES), Polarization (EPL), Repulsive (ERE), Charge Transfer (ECT) and Dispersion (EDI) Terms of the Potential Energy (kcal/mol) Computed for the Subsystem Formed by the Amide N_1H Group and the Adt Rings Generating the Cavity Shown in Figure 5

	EES	EPL	ERE	ECT	EDI
$N_1H\cdots Adt^{**}$	−1.4	−0.5	2.2	−1.2	−2.1
$N_1H\cdots Adt$	−0.5	−0.3	0.6	−0.3	−1.0
$N_1H\cdots Adt^{*}$	−0.5	−0.3	0.6	−0.5	−1.0

The unstarred, single- and double-starred Adt rings are shown in Figure 5 and their equivalent positions are given in Table 5.

The different crystal packing found here for Boc-Adt-Adt-NHMe (**1**), compared with that of its carba-analogue Boc-Ac_5c-Ac_5c-NHMe, needs further consideration. As already observed, both peptides contain two consecutive C^{α}-tetrasubstituted residues which promote a β-turn conformation. However, the propensity of the Ac_5c and Adt residues to fold into 3_{10}-helices is different. In fact, 3_{10}-helices have been demonstrated to occur for Ac_5c homo-polypeptides by x-ray diffraction [37], their formation being favoured by consecutive intramolecular $1 \leftarrow 4$ H-bonds and their aggregation by hydrophobic interactions among the apolar side chains of adjacent chains. At variance, for Adt homo-polypeptides, the helical chain may be destabilized by the lack of consecutive intramolecular $1 \leftarrow 4$ H-bonds. This effect can be the consequence of a different situation arising during the aggregation process. Here, the electron-rich disulfide bridges of the side chains belonging to adjacent backbones may face each other and give rise to unfavourable interactions. These repulsions can be overcome by interactions of the NH groups with the neighbouring disulfide bridges in a manner similar to that found in the crystal packing motif shown in Figure 5. This arrangement, however, prevents the involved NH groups from giving regular, consecutive $1 \leftarrow 4$ H-bonds and may represent a destabilizing mechanism for helical formation by the Adt homo-polypeptides. It is worth noting here that, as shown in Figure 5 and as demonstrated by the above reported calculations, favourable NH···S interactions can efficiently counterbalance unfavourable contacts such as that between the sulfur atoms $^{*}S_1^{\gamma 1}$ and $^{**}S_2^{\gamma 2}$ of 3.425(4) Å that is shorter than the sum of the van der Waals radii.

CONCLUSIONS

Despite the peculiar structure and the chemical reactivity of 1,2-dithiolanes, only very few peptide models containing this heterocyclic ring have been synthesized and structurally characterized [8–11, 17]. This paper reports 3D-structural data concerning the

first linear peptide model **1** containing two consecutive Adt residues. The results clearly show that compound **1** maintains the folding tendency exhibited by the previously studied [18] carba-analogue Boc-Ac_5c-Ac_5c-NHMe and adopts in the crystal a type-III (III′) β-turn conformation stabilized by an intramolecular $1 \leftarrow 4$ H-bond. An analogous folding is preferred in $CHCl_3$ solution.

Furthermore, the presence in this peptide of two consecutive Adt residues, each containing a disulfide bridge, may give rise to a new electron-rich area involving a peculiar type of interaction. This phenomenon is revealed by the aggregation motif found in the crystal packing which shows that the disulfide bridges belonging to different molecules face each other forming a cavity. Moreover, one of the backbone NH group interacts with the cavity sulfur atoms so as to relieve electrostatic repulsion among them. This interaction, in turn, does not allow any C═O···H–N H-bond formation for this NH group. However, the type-III β-turn conformation found in the carba analogue Boc-Ac_5c-Ac_5c-NHMe is maintained, since the NH group involved in the NH···S interactions is not engaged in the $1 \leftarrow 4$ H-bond. At the homo-polypeptide level, the helix structure may be destabilized by the periodical lack of intramolecular C═O···H–N H-bonds. In fact, the unfavourable interactions due to the facing of the disulfide bridges of different helices can be overcome by the NH groups forming NH···S interactions analogous to those observed in the crystal of the Adt peptide reported in this paper.

Taken together, the present and previous findings concerning the Adt residue indicate the promising potential offered by this unusual C^{α}-tetrasubstituted α-amino acid in the production of new synthetic peptides possessing both specific chemical reactivity and a tendency to adopt a well defined conformation. Further studies are in progress in our laboratory to further define these properties.

Acknowledgements

Thanks are due to Professor Giancarlo Fabrizi, University of Rome 'La Sapienza', for useful discussion on NOESY experiments.

REFERENCES

1. Spatola AF. Peptide backbone modifications. A structure–activity analysis of peptides containing amide bond surrogates, conformational constraints, and related backbone replacements. In *Chemistry and Biochemistry of Amino Acids. Peptides, and Proteins*, vol.7, Weinsten B (ed.). Dekker: New York, 1983; 267–357.
2. Hruby VJ, Al-Obeidi F, Kazmierski W. Emerging approaches in the molecular design of receptor-selective peptide ligands: conformational, topographical and dynamic considerations. *Biochem. J.* 1990; **268**: 249–262.
3. Toniolo C, Crisma M, Formaggio F, Peggion C. Control of peptide conformation by the Thorpe-Ingold effect (C^{α}-tetrasubstitution). *Biopolymers (Peptide Sci.)* 2001; **60**: 396–419.
4. Torrini I, Paglialunga Paradisi M, Pagani Zecchini G, Lucente G, Gavuzzo E, Mazza F, Pochetti G, Traniello S, Spisani S. Synthesis, conformation, and biological activity of two fMLP-OMe analogues containing the new 2-[2′-(methylthio)ethyl]methionine residue. *Biopolymers* 1997; **42**: 415–426.
5. Vijayalakshmi S, Balaji Rao R, Karle IR, Balaram P. Comparison of helix-stabilizing effects of α,α-dialkyl glycines with linear and cycloalkyl side chains. *Biopolymers* 2000; **53**: 84–98.
6. Saviano M, Iacovino R, Menchise V, Benedetti E, Bonora GM, Gatos M, Graci L, Formaggio F, Crisma M, Toniolo C. Conformational restriction through $C^{\alpha}{}_i$–$C^{\alpha}{}_i$ cyclization: $Ac_{12}c$, the largest cycloaliphatic $C^{\alpha,\alpha}$-disubstituted glycine known. *Biopolymers* 2000; **53**: 200–212.
7. Formaggio F, Peggion C, Crisma M, Toniolo C, Tchertanov L, Guilhem J, Mazaleyrat J-P, Goubard Y, Wakselman M. A chirally stable, atropoisomeric, C^{α}-tetrasubstituted α-aminoacid: incorporation into model peptides and conformational preference. *Helv. Chim. Acta* 2001; **84**: 481–501.
8. Morera E, Nalli M, Pinnen F, Rossi D, Lucente G. 4-Amino-1,2-dithiolane-4-carboxylic acid (Adt) as cysteine conformationally restricted analogue. Synthetic protocol for Adt containing peptides. *Bioorg. Med. Chem. Lett.* 2000; **10**: 1585–1588, and references cited therein.
9. Morera E, Lucente G, Ortar G, Nalli M, Mazza F, Gavuzzo E, Spisani S. Exploring the interest of 1,2-dithiolane ring system in peptide chemistry. Synthesis of a chemotactic tripeptide and x-ray crystal structure of a 4-amino-1,2-dithiolane-4-carboxylic acid derivative. *Bioorg. Med. Chem.* 2002; **10**: 147–157.
10. Morera E, Pinnen F, Lucente G. Synthesis of 1,2-dithiolane analogues of leucine for potential use in peptide chemistry. *Org. Lett.* 2002; **4**: 1139–1142.
11. Aschi M, Lucente G, Mazza F, Mollica A, Morera E, Nalli M, Paglialunga Paradisi M. Peptide backbone folding induced by the C^{α}-tetrasubstituted cyclic α-amino acids 4-amino-1,2-dithiolane-4-carboxylic acid (Adt) and 1-aminocyclopentane-1-carboxylic acid (Ac_5c). A joint computational and experimental study. *Org. Biomol. Chem.* 2003; **1**: 1980–1988.
12. Teuber L. Naturally occurring 1,2-dithiolanes and 1,2,3-trithianes. Chemical and biological properties. *Sulfur Reports* 1990; **9**: 257–349.
13. Singh R, Whitesides GM. Degenerate intermolecular thiolate-disulfide interchange involving cyclic five-membered disulfides is faster by $\sim 10^3$ than that involving six- or seven-membered disulfides. *J. Am. Chem. Soc.* 1990; **112**: 6304–6309.
14. Hong SY, Jacobia SJ, Packer L, Patel MS. The inhibitory effects of lipoic compounds on mammalian pyruvate dehydrogenase complex and its catalytic components. *Free Radic. Biol. Med.* 1999; **26**: 685–694.
15. Shen T-Y, Walford GL. USP 3,547,948. 1970; *Chem. Abstr.* 1971; **75**: 6336j.
16. Coulter AW, Lombardini JB, Sufrin JR, Talalay P. Structural and conformational analogues of L-methionine as inhibitors of the enzymatic synthesis of *S*-adenosyl-L-methionine. III. Carbocyclic and heterocyclic amino acids. *Mol. Pharmacol.* 1974; **10**: 319–334.
17. Appleton DR, Copp BR. Kottamide E, the first example of a natural product bearing the amino acid 4-amino-1,2-dithiolane-4-carboxylic acid (Adt). *Tetrahedron Lett.* 2003; **44**: 8963–8965.
18. Bardi R, Piazzesi AM, Toniolo C, Sukumar M, Balaram P. Stereochemistry of peptides containing 1-aminocyclopentanecarboxylic acid (Acc^5): solution and solid-state conformations of Boc-Acc^5-Acc^5-NHMe. *Biopolymers* 1986; **25**: 1635–1644.
19. Burla MC, Camalli M, Carrozzini B, Cascarano GL, Giacovazzo C, Polidori G, Spagna R. SIR 2002: the program (2003) *J. Appl. Crystallogr.* 2003; **36**: 1103.
20. Frisch MJ, Pople JA, Binkley J. Self-consistent molecular orbital methods 2S. Supplementary functions for Gaussian basis sets. *J. Chem. Phys.* 1984; **80**: 3265–3269.

21. Morokuma K. Why do molecules interact? The origin of electronic donor-acceptor complexes, hydrogen bonding and proton affinity. *Acc. Chem. Res.* 1977; **10**: 294–300.
22. Boys SF, Bernardi F. The calculation of small molecular interactions by the differences of separate total energies. Some procedures with reduced errors. *Mol. Phys.* 1970; **19**: 553–566.
23. Schmidt MW, Baldridge KK, Boatz JA, Elbert ST, Gordon MS, Jensen JJ, Koseki S, Matsunaga N, Nguyen KA, Su S, Windus TL, Dupuis M, Montgomery JA. General atomic and molecular electronic structure system. *J. Comput. Chem.* 1993; **14**: 1347–1363.
24. Neméthy G, Printz MP. The γ-turn, a possible folded conformation of the polypeptide chain. Comparison with the β-turn. *Macromolecules* 1972; **5**: 755–758.
25. Cung MT, Marraud M, Néel J. Étude expérimentale de la conformation de molecules dipeptidiques. Comparaison avec les prévisions théoriques. *Ann. Chim. (France)* 1972; **7**: 183–209, and references cited therein.
26. Bonora GM, Mapelli C, Toniolo C, Wilkening RR, Stevens ES. Conformational analysis of linear peptides: 5. Spectroscopic characterization of β-turns in Aib-containing oligopeptides in chloroform. *Int. J. Biol. Macromol.* 1984; **6**: 179–188.
27. Rablen PR, Lockman JW, Jorgensen WL. Ab initio study of hydrogen-bonded complexes of small organic molecules with water. *J. Phys. Chem. A* 1998; **102**: 3782–3797, and references cited therein.
28. Venkatachalam CM. Stereochemical criteria for polypeptides and proteins. V. Conformation of a system of three linked peptide units. *Biopolymers* 1968; **6**: 1425–1436.
29. Crisma M, Valle G, Toniolo C, Prasad S, Rao RB, Balaram P. β-Turn conformations in crystal structures of model peptides containing α,α-di-*n*-propylglycine and α,α-di-*n*-butylglycine. *Biopolymers* 1995; **35**: 1–9.
30. Cirilli M, Coiro VM, Di Nola A, Mazza F. Relationship between conformation and geometry as evidenced by molecular dynamics simulation of $C^{\alpha,\alpha}$-dialkylated glycines. *Biopolymers* 1988; **46**: 239–244.
31. Ashida T, Tsunogae Y, Tanaka I, Yamane T. Peptide chain structure parameters, bond angles and conformational angles from the Cambridge structural data-base. *Acta Crystallogr.* 1987; **B43**: 212–218.
32. Benedetti E, Pedone C, Toniolo C, Némethy G, Pottle MS, Scheraga HA. Preferred conformation of the *tert*-butoxycarbonyl amino group in peptides. *Int. J. Peptide Protein Res.* 1980; **16**: 156–172.
33. Toniolo C. $C^{\alpha,\alpha}$-symmetrically disubstituted glycines: useful building blocks in the design of conformationally restricted peptides. *Janssen Chim. Acta* 1993; **11**: 10–16.
34. Mahmud S, Davidson ER. Theoretical study of the absorption of carbon monoxide on a NaCl surface. *Surf. Sci.* 1995; **322**: 342–360.
35. Hertwig R, Koch W, Schroder D, Schwarz H, Hrusak J, Schwerdtfeger P. A comparative computational study of cationic coinage metal-ethylene complexes $(C_2H_4)M^+$ (M = Cu, Ag, and Au). *J. Phys. Chem.* 1996; **100**: 12 253–12 260.
36. Aschi M, Mazza F, Di Nola A. Cation-π interactions between ammonium ion and aromatic rings: an energy decomposition study. *J. Mol. Struct. (THEOCHEM)* 2002; **587**: 177–188.
37. Santini A, Barone V, Bavoso A, Benedetti E, DiBlasio B, Fraternali F, Lelj F, Pavone V, Pedone C, Crisma M, Bonora GM, Toniolo C. Structural versatility of peptides from $C^{\alpha,\alpha}$-dialkylated glycines: a conformational energy calculation and x-ray diffraction study of homopeptides from 1-aminocyclopentane-1-carboxylic acid. *Int. J. Biol. Macromol.* 1988; **10**: 292–299.